



University  
of Glasgow

Streicker, D., Winternitz, J. C., Satterfiled, D. A., Condori-Condori, R. E., Broos, A., Tello, C., Recuenco, S., Velasco-Villa, A., Altizer, S., and Valderrama, W. (2016) Host-pathogen evolutionary signatures reveal dynamics and future invasions of vampire bat rabies. *Proceedings of the National Academy of Sciences of the United States of America*, 113(39), pp. 10926-10931. (doi:10.1073/pnas.1606587113)

There may be differences between this version and the published version. You are advised to consult the publisher's version if you wish to cite from it.

<http://eprints.gla.ac.uk/121483/>

Deposited on: 28 July 2016

Enlighten – Research publications by members of the University of Glasgow  
<http://eprints.gla.ac.uk>

# Host-pathogen evolutionary signatures reveal dynamics and future invasions of vampire bat rabies

Daniel G. Streicker<sup>a,b,c,1</sup>, Jamie Winternitz<sup>c,d,e</sup>, Dara Satterfield<sup>c</sup>, Rene Edgar Condori-Condori<sup>f</sup>, Alice Broos<sup>b</sup>, Carlos Tello<sup>g</sup>, Sergio Recuenco<sup>h</sup>, Andres Velasco-Villa<sup>f</sup>, Sonia Altizer<sup>c</sup> and William Valderrama<sup>g</sup>

<sup>a</sup> Institute of Biodiversity, Animal Health and Comparative Medicine, University of Glasgow, Glasgow, G12 8QQ, Scotland, UK <sup>b</sup> MRC-University of Glasgow Centre for Virus Research, Glasgow, G61 1QH, Scotland, UK <sup>c</sup> Odum School of Ecology, University of Georgia, Athens, GA 30602, USA <sup>d</sup> Institute of Vertebrate Biology, Czech Academy of Sciences, v.v.i., Květná 8, 603 65 Brno, Czech Republic <sup>e</sup> Department of Evolutionary Ecology, Max Planck Institute for Evolutionary Biology, 24306 Ploen, Germany <sup>f</sup> Poxvirus and Rabies Branch, Division of High Consequence Pathogen and Pathology, Centers for Disease Control and Prevention, Atlanta, GA 30606, USA <sup>g</sup> Association for the Conservation and Development of Natural Resources, Lima, Peru <sup>h</sup> Instituto Nacional de Salud, Ministry of Health of Peru, Lima, Peru

Submitted to Proceedings of the National Academy of Sciences of the United States of America

**Anticipating how epidemics will spread across landscapes requires understanding host dispersal events that are notoriously difficult to measure. Here, we contrast host and virus genetic signatures to resolve the spatiotemporal dynamics underlying geographic expansions of vampire bat rabies virus (VBRV) in Peru. Phylogenetic analysis revealed recent viral spread between populations that, according to extreme geographic structure in maternally-inherited host mitochondrial DNA, appeared completely isolated. In contrast, greater population connectivity in bi-parentally inherited nuclear microsatellites explained the historical limits of invasions, suggesting that dispersing male bats spread VBRV between genetically isolated female populations. Host nuclear DNA further indicated unanticipated gene flow through the Andes mountains connecting the VBRV-free Pacific coast to the VBRV-endemic Amazon rainforest. By combining Bayesian phylogeography with landscape resistance models, we projected invasion routes through northern Peru that were validated by real-time livestock rabies mortality data. The first outbreaks of VBRV on the Pacific coast of South America could occur by June 2020, which would have serious implications for agriculture, wildlife conservation and human health. Our results show that combining host and pathogen genetic data can identify sex-biases in pathogen spatial spread, which may be a widespread but underappreciated phenomenon, and demonstrate that genetic forecasting can aid preparedness for impending viral invasions.**

Desmodus | zoonotic disease | forecasting | sex bias | spatial dynamics

Knowledge of the mechanisms governing the spread of pathogens across landscapes is vital to predict disease emergence in humans, domestic animals and wildlife (1). The spread of directly transmitted pathogens is intimately linked to host dispersal, but for most wildlife hosts, actively tracking the movements of infected individuals is logistically impractical at pertinent temporal and spatial scales (2). Indirect population genetic methods overcome this limitation by characterizing historical patterns of dispersal in host genomes, raising the possibility that host genetic structure could forecast the pathways of invading pathogens. However, host genetic structure may not correlate with pathogen spread because of different timescales reflected in host and pathogen genomes or if infection alters host dispersal behavior (3, 4). Differences among genomes in modes of inheritance might also influence genetic forecasts of pathogen spread. Bi-parentally inherited host nuclear DNA (nuDNA) reveals the joint population structure of both sexes, whereas maternally-inherited mitochondrial DNA (mtDNA) indicates female population structure. Incongruence between host genomes is commonly attributed to sex-biases in dispersal and/or differences in rates of lineage sorting (5, 6). In contrast, pathogen genomes are transmitted horizontally between hosts and often evolve on

rapid timescales, providing high-resolution markers of the contemporary movements of infected individuals of both sexes (4). Therefore, congruence of pathogen population structure to host nuDNA or mtDNA population structure, but incongruence to the other, could identify which host genome is most relevant to epidemic spread while signaling a potentially sex-linked mechanism of pathogen dispersal.

Here, we apply nuclear, mitochondrial and viral genetic markers to explore the spatial spread of vampire bat (*Desmodus rotundus*) rabies virus (VBRV; *Lyssavirus*, *Rhabdoviridae*), a directly transmitted zoonosis that causes universally fatal encephalitis when infected bats feed on livestock and humans (7). VBRV is a constant impediment to public health and agriculture in Latin America, with annual costs exceeding US\$30 million in livestock mortality alone (8). Control programs focus on reducing the size of bat populations using topical anticoagulant poisons (7). However, because long-term viral maintenance depends more strongly on viral dispersal between vampire bat colonies than on colony size, decades of culling have failed to eliminate VBRV (9, 10). Instead, human and livestock VBRV mortality are increasing and the virus is emerging in historically VBRV-free areas throughout Latin America (7, 11). Linking patterns of bat dispersal to viral spread is therefore essential to improve disease control in endemic areas and to predict pathways of ongoing invasions.

## Significance

**In Latin America, vampire bat rabies constrains livestock production and is the main cause of lethal human rabies outbreaks. Despite knowledge that bat dispersal prevents viral extinction and compromises control campaigns, the movement patterns of infected bats are unknown. Using large host and virus datasets, we illustrate a genetic approach to link population level patterns of host dispersal to pathogen spatial spread that overcomes logistical limitations of tracking animal movement in the wild. Results implicate male vampire bats as contributing disproportionately to rabies spatial spread and offer new opportunities to forecast and prevent rabies. The ubiquity of sex-biased dispersal in animals suggests sex-biased pathogen spread could widely influence the distribution and invasion dynamics of emerging diseases.**

## Reserved for Publication Footnotes

137  
138  
139  
140  
141  
142  
143  
144  
145  
146  
147  
148  
149  
150  
151  
152  
153  
154  
155  
156  
157  
158  
159  
160  
161  
162  
163  
164  
165  
166  
167  
168  
169  
170  
171  
172  
173  
174  
175  
176  
177  
178  
179  
180  
181  
182  
183  
184  
185  
186  
187  
188  
189  
190  
191  
192  
193  
194  
195  
196  
197  
198  
199  
200  
201  
202  
203  
204

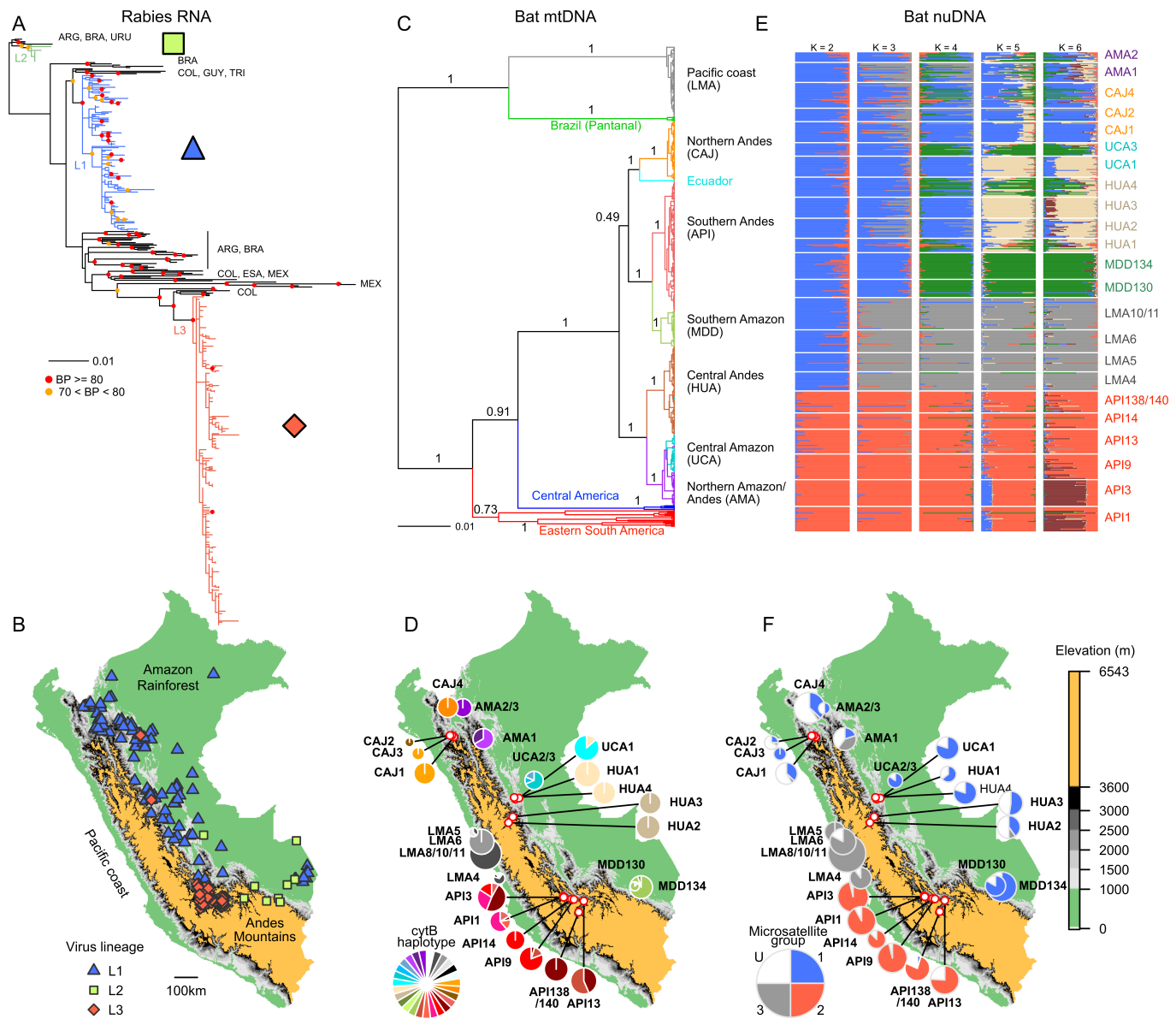


**Fig. 1. Genetic and geographic structure of host and viral markers with distinct inheritance mechanisms.** A) The ML tree of VBRV, using 434 complete *N* sequences from Peru (colored branches) and other representative countries in the Americas (black branches; ARG = Argentina, BRA = Brazil, COL = Colombia, ESA = El Salvador, GUY= French Guiana, MEX = Mexico, TRI= Trinidad, URU = Uruguay). Colored symbols show bootstrap support from 1000 replicate ML searches. Two outgroup sequences from a rabies variant circulating in Peruvian dogs were excluded for visualization. B) Geographic distributions of viral lineages in Peru. Areas above 3600 meters (the upper limit to vampire bats in Peru) are colored gold. C) Bayesian phylogenetic tree of *cytB* sequences from vampire bats from Peru (*N* = 442) and other countries in the Americas (*N* = 26). Branches are colored by geographic region. Node values are posterior probabilities. D) Distribution of *CytB* haplotypes across vampire bat colonies in Peru. Sites with < 8 sequenced individuals were grouped with other colonies surveyed within 10km. Pie charts are proportionate to sample size (range = 8 - 30). E) Estimates from STRUCTURE analyses assuming *K* = 2 - 6 populations using 9 microsatellites (*N* = 480 bats). Each bar represents the probability of membership assignment to each of *K* groups. F) Pie charts show the distribution of microsatellite groups (*K* = 3, threshold probability for group membership = 0.85, un-assigned individuals in white).

Prior population genetic studies concluded that the low vagility and small home range sizes of vampire bats generate high genetic differentiation among populations (12, 13). However, genetic lineages of VBRV are geographically widespread, implying that the virus overcomes the genetic isolation of its host through a currently unidentified dispersal mechanism (14, 15). In carnivores, non-resident, nomadic individuals and seasonal variation in contact networks are thought to influence pathogen prevalence within populations, but the role of host social structure on pathogen spread at larger spatial scales is less understood (16, 17). Like most mammals, male vampire bats disperse upon sexual maturity, while females retain strong fidelity to the na-

tal roost (18, 19). We therefore hypothesized that male-biased dispersal could spread VBRV between colonies, giving males a pivotal role in the regional persistence and spatial propagation of outbreaks across landscapes. As male dispersal contributes to nuclear but not mitochondrial gene flow, we predicted that bat nuclear population structure would explain historical invasions of VBRV. Further, since male dispersal may be prompted by the subsequent year's annual birth pulse (19), we hypothesized that expansions could be seasonal. Finally, we tested whether linking simple landscape resistance models with viral phylogeography can forecast rates and routes of viral invasion to currently VBRV-free regions. We realize these objectives using datasets representing

205  
206  
207  
208  
209  
210  
211  
212  
213  
214  
215  
216  
217  
218  
219  
220  
221  
222  
223  
224  
225  
226  
227  
228  
229  
230  
231  
232  
233  
234  
235  
236  
237  
238  
239  
240  
241  
242  
243  
244  
245  
246  
247  
248  
249  
250  
251  
252  
253  
254  
255  
256  
257  
258  
259  
260  
261  
262  
263  
264  
265  
266  
267  
268  
269  
270  
271  
272

273  
274  
275  
276  
277  
278  
279  
280  
281  
282  
283  
284  
285  
286  
287  
288  
289  
290  
291  
292  
293  
294  
295  
296  
297  
298  
299  
300  
301  
302  
303  
304  
305  
306  
307  
308  
309  
310  
311  
312  
313  
314  
315  
316  
317  
318  
319  
320  
321  
322  
323  
324  
325  
326  
327  
328  
329  
330  
331  
332  
333  
334  
335  
336  
337  
338  
339  
340

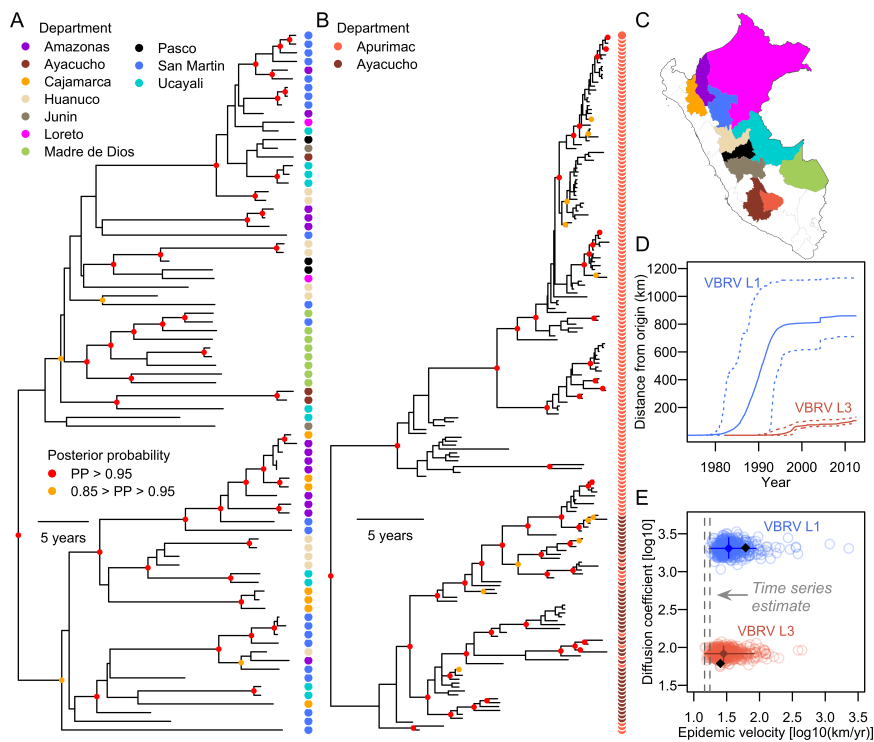


**Fig. 2. Dynamics of historical viral dispersal within Peru.** Bayesian phylogenetic trees of VBRV L1 (A) and L3 (B), with tip symbols colored according to Department of Peru (C). Inner node symbols are posterior probabilities (PP) of clades. D) Spatial expansions of each viral lineage, depicted as the cumulative geographic distance from the inferred outbreak origin through time. E) Posterior distributions of the epidemic velocity and diffusion coefficient of each viral lineage. Points are parameter estimates from the tips of one randomly sampled tree from the posterior distribution of each Bayesian phylogeographic analysis. Solid diamonds and lines are the median and 95% HPDs on parameter estimates, respectively. Black diamonds are median statistics calculated across all branches. Vertical dashed lines are the 95% bounds of the wavefront velocity estimated from time series data in northern Peru (see Fig. 3 and *SI Appendix*, Fig. S9).

341  
342  
343  
344  
345  
346  
347  
348  
349  
350  
351  
352  
353  
354  
355  
356  
357  
358  
359  
360  
361  
362  
363  
364  
365  
366  
367  
368  
369  
370  
371  
372  
373  
374  
375  
376  
377  
378  
379  
380  
381  
382  
383  
384  
385  
386  
387  
388  
389  
390  
391  
392  
393  
394  
395  
396  
397  
398  
399  
400  
401  
402  
403  
404  
405  
406  
407  
408

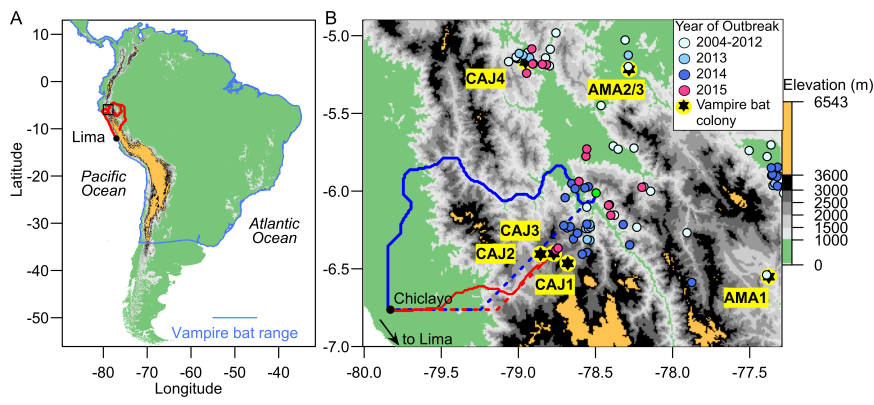


**Fig. 3. Forecasting invasion of VBRV to the Pacific coast of South America.** A) The South American range of vampire bats, colored as in Fig 1. Red lines are least-cost pathways from bat colonies in the Andes and Amazon with MG3 individuals (typical of the coast) to Lima using the “valley” resistance model. The black box indicates the region in panel B. B) Blue lines are least cost routes from the westernmost VBRV outbreak in 2012 (green point) to Chiclayo (a reference point for the Pacific coast) according to the valley (solid) and threshold (dotted) resistance models. Red lines are routes from the western front of the epidemic in 2015. Light blue points (2004-2012) are outbreaks that were included in phylogenetic analyses.

hundreds of host nuclear, host mitochondrial and viral genomes from Peru along with a 13 year spatially-explicit time series on VBRV outbreaks in sentinel livestock.

**Results**

**Viral genetic structure.** We sequenced the complete nucleoprotein (*N*) gene from 264 rabies isolates collected from Peruvian livestock between 1997-2012 and compared these to representative sequences from throughout the Americas. Because livestock infect neither each other nor bats, each isolate represents a single transmission event from bat to livestock, providing a window of insight into locally circulating bat viruses (14, 15). A maximum likelihood (ML) phylogenetic tree revealed three viral lineages in Peru, each of which shared a most recent common ancestor (MRCA) with viruses from other South American countries, consistent with multiple, independent introductions of VBRV into Peruvian bats (Fig. 1A). Two viral lineages, L1 and L2, circulated exclusively east of the Andes mountains and overlapped in the southern and central Amazon (Fig. 1B). Viral lineage 3 (L3) was isolated in inter-Andean valleys in southern Peru, with the excep-

tion of two samples found well outside that range (Fig. 1B). The outlier viruses were paraphyletic to each other (indicating distinct introductions) and were found in rarely infected species (dog and horse), suggesting human-mediated translocations of companion animals, rather than infections acquired from indigenous bats at the sampling locality.

**Contrasting the population structure of vampire bat genomes to rabies virus.** A Bayesian phylogenetic analysis of mitochondrial cytochrome B (*cytB*) sequences from 468 vampire bats showed marked geographic structure. Bats captured west of the Andes mountains in the department of Lima were highly divergent from other Peruvian bats and were more closely related to bats from south-western Brazil (Fig. 1C). Bats east of the Andes formed a separate monophyletic group (with a single sequence from Ecuador) that shared a most recent common ancestor (MRCA) with populations in Central America (posterior probability, PP = 0.91). Most mitochondrial lineages were found exclusively within single Departments (equivalent to US States) of Peru (Fig. 1C). In some cases (e.g., AMA and CAJ), colonies separated by short distances were comprised exclusively of individuals from distinct



409 and paraphyletic mitochondrial lineages, indicating a lack of  
410 female gene flow among nearby colonies since lineages diverged.  
411 A lineage found in both the central Amazon (UCA sites) and  
412 the northern Amazon (AMA sites) was a potential exception;  
413 however, the well supported sub-clades within this lineage were  
414 restricted to either UCA or AMA, but not both (Fig. 1C, *SI*  
415 *Appendix*, Fig. S6). Spatial isolation was even stronger at the  
416 haplotype level. Of 27 haplotypes, 16 were exclusive to single  
417 bat colonies and the mean distance occupied by haplotypes was  
418 only 22km (range = 0 – 258.1km). Minimal sharing of haplotypes  
419 between distant colonies implied the absence of contemporary  
420 mitochondrial gene flow between regions (Fig. 1D).

421 We next compared the population structure of bi-parentally  
422 inherited nuclear markers to that of mtDNA and viral RNA.  
423 Nine nuclear microsatellites from 480 vampire bats indicated 2-  
424 3 genetic groups (K), with admixture among all colonies east of  
425 the Andes (microsatellite group 1, MG1, Fig. 1E-F) and genetic  
426 isolation of vampire bat colonies found in inter-Andean valleys in  
427 southern Peru (API sites, microsatellite group 2, MG2). At  $K >$   
428 2, bats from the Pacific coast (LMA sites) formed a distinct group  
429 (MG3), which was also detected at low to moderate frequency  
430 in the northern Andes and Amazon (Fig. 1E). These findings  
431 were robust to analysis of only 6 loci without null alleles, two  
432 alternative methods of statistical inference (STRUCTURE and  
433 DAPC), and to relaxing priors on the spatial locations of sampled  
434 bat populations (*SI Appendix*, Fig. S2-S4). Larger (less plausible)  
435 values of K revealed additional geographic clusters but implied  
436 extensive gene flow among them (Fig. 1E), an expected pattern  
437 given the isolation by distance in our microsatellite data (*SI*  
438 *Appendix*, Fig. S5). Importantly, even at the highest levels of K,  
439 microsatellite groups spanned areas east of the Andes, providing  
440 a potential corridor for viral spread through the Amazon and  
441 eastern slopes of the Andes.

442 We assessed individual-level genomic mismatches between  
443 nuDNA and mtDNA using 352 bats for which we had both  
444 microsatellite and mitochondrial data. Bats east of the Andes  
445 carried highly divergent mtDNA lineages, but belonged to the  
446 same microsatellite group (*SI Appendix*, Fig. S6). Therefore, viral  
447 lineages L1 and L2 were maintained by MG1 bats with diverse and  
448 paraphyletic mitochondrial haplotypes, whereas L3 exclusively  
449 infected MG2 bats with API mitochondrial haplotypes, creat-  
450 ing viral genetic congruence to nuDNA, but not mtDNA. The  
451 atypical MG3 bats found in the Andes and Amazon had locally  
452 prevalent mtDNA haplotypes, suggesting that male immigrants  
453 from the coast reproduce with resident females despite the long  
454 branch separating these populations in the *cytB* phylogeny (Fig.  
455 1C).

456 **Microsatellite confirmation of male-biased dispersal.**  
457 Greater structure in maternally inherited markers relative  
458 to nuclear markers signaled the expected pattern of female  
459 philopatry and male-biased dispersal (19, 20). Additional tests  
460 using microsatellites found a nearly 14-fold increase in the  
461  $F_{IS}$  of male vampire bats relative to females (female  $F_{IS} =$   
462  $-0.0003$ , male  $F_{IS} = 0.1363$ ,  $P < 0.0004$ ), consistent with the  
463 expectation that the dispersing sex should have heterozygote  
464 deficiency since samples represent a mixture of populations (i.e.,  
465 the Wahlund effect) (21). Other genetic comparisons of males  
466 and females were not statistically significant (*SI Appendix*, Table  
467 S7), but detection by any one of the above methods implies  
468 intense sex-biased dispersal (21). Similarly, using the assignment  
469 probabilities from our STRUCTURE analysis, we found that  
470 putative recent migrants ( $PP < 0.2$  for belonging to the locally  
471 abundant genotype group) tended to be male (59.3% for all  
472 Peru, 65.2% for bats within the range of MG1).

473 **Seasonal expansions of rabies across the landscape.** We  
474 estimated the monthly area of Peru infected by VBRV from  
475 2003-2014 using a database of 1146 laboratory-confirmed live-

476 stock rabies outbreaks (11). Time series decomposition revealed  
477 significant seasonality in the area infected (generalized additive  
478 model: deviance explained = 27.7%,  $p < 0.001$ ) with peak spatial  
479 expansions in November and December (*SI Appendix*, Fig. S10).

480 **Reconstructing and forecasting viral invasion dynamics.**  
481 Having identified congruence between bat nuDNA and viral  
482 geographic distributions as a potential by-product of male-biased  
483 dispersal, we sought to reconstruct and forecast the dynamics  
484 of viral spread across the landscape. We applied Bayesian con-  
485 tinuous phylogenetic ancestral state estimation to L1 and L3  
486 viruses with precisely known collection dates and GPS locations  
487 ( $N_{L1} = 81$ ,  $N_{L3} = 179$ ). To enhance phylogenetic resolution, we  
488 added sequence data from the hypervariable, non-coding region  
489 between the glycoprotein and polymerase genes (G-L, 510bp)  
490 to the complete *N* gene sequences. Similar analyses of lineage  
491 L2 were precluded by low sample size and the disappearance  
492 of this virus after 2009 (*SI Appendix*, Table S8). However, the  
493 lack of genetic isolation by geographic distance in available data  
494 suggests relatively unconstrained dispersal of that virus during its  
495 tenure in Peru (*SI Appendix*, Fig. S7). Phylogeographic models  
496 showed viral invasions occurred within the past 40 years (L1: 95%  
497 Highest Posterior Density [HPD] on MRCA = 20.65 – 35.02; L3:  
498 95% HPD = 16.27 – 28.0). Although some geographic clustering  
499 was apparent in both viral lineages, jumps between the Peruvian  
500 Departments within the range of each lineage were common  
501 (Fig. 2AB). Both viruses underwent decelerating invasions, with  
502 initially rapid increases in geographic extent followed by gradual  
503 expansions in the last 10-15 years (Fig. 2D). The greater spatial  
504 scale of historical expansions of L1 produced a higher median  
505 velocity in L1 compared to L3 (61.5 [95% HPD = 26.2 – 194.5] vs  
506 25.4 [95% HPD = 14.9 – 50.1] km/year). However, contemporary  
507 velocities calculated from tip branches (1997 – 2012) were similar  
508 between lineages (L1: 33.9 vs L3: 28.4 km/yr, Fig. 2E).

509 Unexpected gene flow of MG3 from the rabies-free Pacific  
510 coast to the rabies-endemic Andes and Amazon prompted us to  
511 explore corridors for viral invasion to the Pacific coast of South  
512 America (Fig. 1F, *SI Appendix*, Fig. S6). A landscape resistance  
513 model describing the well known pattern of VBRV spread along  
514 valleys (7, 11), showed least-cost routes from Andean and Ama-  
515 zonian bat colonies with MG3 individuals to the coast passed  
516 through a corridor in the north of Peru that forms the lowest  
517 pass throughout the length of the Andes (the Huancabamba  
518 Depression, Fig. 3A). We projected the invasion of VBRV by  
519 combining phylogeographic estimates of viral dispersal velocities  
520 with least cost distances to the coast. Assuming velocities inferred  
521 from the tips of L1 and L3 phylogenies, respectively, we forecast  
522 the arrival of VBRV to Chiclayo (a major city on the coast) by  
523 July 2019 (95% HPD: 2016.85 – 2023.25) or June 2020 (95%  
524 HPD: 2017.12 – 2024.93). Rabies mortality data from livestock  
525 during the 3 years after our viral sequence data were collected  
526 (2013-2015) confirmed ongoing viral invasion along the routes  
527 projected by landscape resistance models (Fig. 3B). These non-  
528 genetic data show that VBRV travelled 50.1km southwest from  
529 June 2012 to April 2015 at 16.1km/yr (95% CI = 14.6 – 17.6, Fig.  
530 2E, *SI Appendix*, Fig. S9), leaving less than 145km to the Pacific  
531 coast of South America.

## 532 Discussion

533 By combining large host and virus genetic datasets, we show  
534 female philopatry and male-biased dispersal in vampire bats likely  
535 creates a disproportionate role for male bats in the spatial spread  
536 of VBRV. Using these insights on host and virus dispersal, we  
537 forecast routes and rates of an ongoing viral invasion that we pre-  
538 dict will cause an historic and damaging first invasion of VBRV to  
539 the Pacific coast of South America. Independent epidemiological  
540 data support our genetic predictions.

545 Reduced host population structure in nuclear relative to  
546 mitochondrial markers and heterozygote deficiency in males are  
547 consistent with male dispersal and female philopatry in vampire  
548 bats, as is known from field studies and is the general expectation  
549 for mammals (18, 19). We suggest that a by-product of sex-biased  
550 dispersal is that the spatial spread and geographic distribution of  
551 VBRV will also be male-driven. Biologically, the long incubation  
552 period (2-4 weeks) and the short infectious period of rabies (2-  
553 3 days) means that most viral dispersal will occur before the  
554 onset of disease (22). Moreover, the debilitating clinical signs of  
555 rabies (ataxia, lethargy and death) during most of the infectious  
556 period make it unlikely that infection could induce unusually long  
557 distance dispersal in infected females, thereby spreading VBRV  
558 without leaving a mtDNA signature of dispersal through repro-  
559 duction. Therefore, the sex that disperses most while incubating  
560 rabies (males) will naturally dominate viral spread, and barriers  
561 to male dispersal will delimit the boundaries of viral distributions,  
562 as we observed. The seasonality in the geographic area infected by  
563 VBRV was also consistent with male-biased spatial spread. Viral  
564 expansions peaked at the start of the wet season (*SI Appendix*, Fig.  
565 S10), when a new cohort of births is expected to initiate dispersal  
566 of males from the previous year (19, 23). This provides indirect  
567 evidence for pulses of VBRV expansion driven by seasonal male  
568 bat dispersal, though other seasonal and non-seasonal factors  
569 could also influence spatial expansions.

570  
571 In principle, incongruence between host genomes could arise  
572 from limitations of genetic data examined here; however, several  
573 lines of evidence argue against this interpretation. First, rates of  
574 lineage sorting and mutation differ between nuDNA and mtDNA  
575 and imply different timescales of population structure (6). Given  
576 that viral invasions occurred within the last 40 years, we are  
577 most concerned with contemporary bat population structure as  
578 revealed by microsatellites (which matched the viral distribu-  
579 tion) and the landscape distribution of mtDNA haplotypes. If  
580 contemporary dispersal were equal among sexes and the pat-  
581 terns we observed arose from different genetic timescales, we  
582 would have expected mtDNA haplotypes to span epidemiologi-  
583 cally connected regions, rather than being most often restricted  
584 to single bat colonies. The number or power of microsatellites  
585 also cannot explain their weaker population structure relative to  
586 mtDNA. Both six and nine microsatellites differentiated API bats  
587 from MDD bats, despite their close relatedness in the mtDNA  
588 phylogeny (Fig. 1C), and simulations showed 98-100% power to  
589 detect population structure (*SI Appendix*, Fig. S8).

590  
591 The ubiquity of sex-biased dispersal in nature (typically fe-  
592 male biased in birds and male biased in mammals (18)) could  
593 make sex-biased pathogen spread a widespread determinant of  
594 epidemic propagation at the landscape level. Sex-biased pathogen  
595 spread is difficult to detect using traditional methods for studying  
596 animal movement such as radio-telemetry or GPS tags because  
597 rare dispersal events that can be critical for disease spread will  
598 be missed in studies carried out over small spatiotemporal scales.  
599 This study shows that contrasting host and pathogen genetic  
600 markers with different inheritance modes provides a framework  
601 to begin to evaluate sex-biased pathogen dispersal. Other ap-  
602 proaches, such as theoretical modeling of pathogen transmission  
603 within host contact networks, incorporate similar concepts, but  
604 typically lack corresponding data from pathogens to verify how  
605 host dispersal heterogeneity affects disease spread, require exten-  
606 sive field datasets on host contacts, and offer limited guidance  
607 for managing pathogens emerging at the landscape level (17,  
608 24). Identifying the sex responsible for pathogen spread carries  
609 practical implications for the prevention and control of VBRV  
610 because blocking viral movement between colonies is predicted  
611 to cause viral extirpation (10). Future work should quantify the  
612 scales at which males and females contribute to inter-colony viral

spread to evaluate the efficacy of targeting dispersing males in  
rabies control campaigns.

615 We also show that combining host population genetics,  
616 pathogen phylogeography and landscape ecology can predict  
617 rates and routes of pathogen invasion to disease-free areas. A  
618 similar approach could be useful to forecast other emerging  
619 pathogen invasions where the lack of long term infection data  
620 precludes traditional epidemiological analyses. Most importantly,  
621 we forecast viral invasion to the historically VBRV-free Pacific  
622 coast of South America (25) via a previously undetected corridor  
623 of vampire bat gene flow across the Peruvian Andes. Three years  
624 of independent livestock rabies mortality data confirmed viral ex-  
625 pansion along comparable routes and velocity to model forecasts  
626 (Fig. 2E, Fig. 3). We caution invasions could accelerate or decel-  
627 erate closer to the coast where landscapes are less complex than  
628 the Andes or Amazon and that alternate routes have not been  
629 excluded. However, at present, we foresee no significant barriers  
630 to continued invasion. Vampire bats occur continuously from the  
631 leading edge of the wavefront to the Pacific coast (26) and VBRV  
632 summited the highest remaining peak in 2015 (Fig. 3B). The  
633 evolutionary divergence of coastal from Andean sub-populations  
634 is also unlikely to stop VBRV as rabies host shifts are common  
635 within bat genera (27) while the subpopulations in question are  
636 inter-breeding (*SI Appendix*, Fig. S6). More work is needed to  
637 determine whether the current invasion was triggered by recent  
638 changes in bat population structure, gradual viral invasion to  
639 the fringes of the vampire bat distribution or a combination.  
640 Regardless of the initiating mechanism, the arrival of VBRV to  
641 the coastal regions of Peru and subsequent potential spread to  
642 Ecuador and northern Chile would be profoundly damaging for  
643 agriculture. The presence of VBRV would also create new risks  
644 to humans that interact with bats or infected livestock and to  
645 wildlife such as sea lions that constitute an important food source  
646 for coastal vampire bats (28). Culling vampire bats failed to stop  
647 advancing VBRV epidemics in Argentina and could conceivably  
648 exacerbate viral spread if culls promote bat dispersal, as was ob-  
649 served in badger culls aiming to control bovine tuberculosis in the  
650 UK (10, 29, 30). We therefore advocate heightened surveillance,  
651 preventative livestock vaccination and educational campaigns to  
652 reduce the burden of impeding epidemics.

653 Previous comparisons of host and pathogen genetic data have  
654 exploited pathogens as a high resolution marker of host demog-  
655 raphy and dispersal or have studied co-evolutionary dynamics  
656 over longer timescales (4, 31). Our study shows that similar data  
657 can verify key host demographic groups for pathogen spatial  
658 spread and forecast epidemic invasions to disease-free areas. As  
659 the abundance and resolution of host and pathogen genomic  
660 data increase, similar approaches could test the generality of sex-  
661 biased pathogen dispersal while providing important foresights  
662 into the landscape dynamics of emerging pathogen invasions.

## 663 Materials and Methods

664 **Vampire bat and rabies virus data.** Biopsies of bat wing membranes were  
665 collected in 2008-2013 from twenty-nine vampire bat colonies across 7  
666 Peruvian Departments in the Pacific coast, Andes mountains and Amazon  
667 rainforest (Table S1). In addition, we acquired 264 rabies-infected livestock  
668 brains from 13 Departments of Peru, collected between 1997-2012 by the  
669 passive surveillance system of the National Service of Agrarian Health of Peru  
670 (SENASA). Further data details and laboratory procedures for sequencing  
671 and genotyping are described in the *SI Appendix*. All sequences have been  
672 deposited to GenBank (*cytB*: KU937964-KU938399, *Rabies virus*: KU938400 -  
673 KU938924).

674 **Viral phylogenetic analyses.** ML phylogenetic trees were estimated with  
675 Garli 2.01 using Peruvian samples with complete *N* gene sequences and  
676 geographic information at least to the district level (32). We included up  
677 to 5 sequences per lineage for VBRVs from other regions of Latin America  
678 and two dog rabies sequences as outgroups. The topology was selected as  
679 the best of 10 replicate ML searches with random starting trees using the  
680 GTR+I+G substitution model. Bootstrap values were calculated from 1000  
681 additional ML searches using the best topology from the first set of searches  
682 as a starting tree. Phylogeographic analyses were carried out in BEAST v.1.8  
683 (33). Preliminary runs indicated use of a lognormal relaxed molecular clock



681 for *N* and a strict molecular clock for *G-L* data for both lineages. Nucleotide  
682 substitution models were selected for codon positions one and two (to-  
683 gether) and for codon position 3 using Akaike's Information Criterion (AIC)  
684 corrected for small sample size in jModeltest 2 (34). Triplicate MCMC chains  
685 were run for 50 million generations, with trees and parameters sampled  
686 every 10,000 steps. We evaluated three relaxed random walk models of  
687 spatial diffusion using Bayes Factors (BF) (35, 36) and present results from the  
688 gamma model in Fig. 2 (BF > 8.5 for gamma vs other models). Convergence  
689 within and across runs and appropriate burn in periods were checked in  
690 Tracer. For L3, the overall likelihood converged, but tree likelihoods for  
691 individual data partitions swapped between competing values throughout  
692 runs regardless of chain lengths. Demographic parameters (TMRCA, diffusion  
693 rate) were uncorrelated with swaps. Diffusion coefficients and dispersal  
694 velocities were estimated from 1000 randomly sampled trees from each  
695 posterior distribution using the *Seraphim* package of R (37).

696 **Host population genetic analyses.** Bayesian phylogenetic analysis of  
697 mitochondrial *Cytb* sequences was performed with BEAST using the HKY+I  
698 model of nucleotide substitution selected by AIC in jModeltest 2, assum-  
699 ing constant effective population size. One sequence of *Diphylla ecaudata*  
700 (Hairy-legged vampire bat, Genbank: DQ077399) was included as an out-  
701 group. Trees were sampled every 1000 states for 20 million generations and  
702 the first 2001 trees were removed prior to generating a maximum clade  
703 credibility tree. *Cytb* haplotypes were designated using the *pegas* package  
704 of R after removing the first 5bp from sequences due to missing data in  
705 some samples (38). Nuclear population structure was assessed with two  
706 classification methods: STRUCTURE (a Bayesian clustering method) minimizes  
707 Hardy-Weinberg and linkage disequilibrium, and DAPC (discriminant analysis  
708 of principal components) identifies genetic clusters that maximize between-  
709 group variance and minimize within-group variance (39, 40). The *SI Appendix*  
710 provides summary statistics on microsatellites, additional checks performed  
711 and details of analyses of host population structure.

712 **Forecasts of viral invasion.** We applied the velocities estimated from  
713 continuous phylogeographic analyses to least cost distances from landscape

714 models of bat dispersal to predict pathways and dates of VBRV spread.  
715 Distances were calculated with 2 landscape models in the *gdistance* package  
716 of R: first a path through any elevation under 3600m ("threshold model")  
717 and second, assuming exponentially increasing costs from 1 to 3600m, with  
718 no dispersal above 3600m ("valley model"). These models qualitatively and  
719 quantitatively capture the observed spread of VBRV epidemics through river  
720 valleys (7, 11). Distances from the leading edge of a westward-expanding  
721 VBRV epidemic (April 2015, La Colca, Department of Cajamarca) to Chi-  
722 clayo differed by only 5.7km between models (136.37 versus 143.32km);  
723 we therefore use the second, more conservative scenario in forecasts. To  
724 confirm ongoing VBRV invasions along the projected route, we analyzed 31  
725 laboratory confirmed rabies outbreaks in livestock that were reported after  
726 our sequence data were collected (2013 – 2015) using the linear regression  
727 technique of ref. (11).

728 **Acknowledgements.** We thank Heather Danaceau, Jennifer Towner and  
729 Victoria Estacio for laboratory assistance and Roman Biek, Barbara Mable  
730 and Mafalda Viana for comments on the manuscript. SENASA contributed  
731 surveillance data and livestock samples under an International Cooper-  
732 ative Agreement with the University of Georgia (30-11-2012). The Per-  
733 uvia Government authorized collection, exportation and use of genetic  
734 resources (RD-222-2009-AG-DGFFS-DGEFFS; 003851-AG-DGFFS, RD-273-201-  
735 2-AG-DGFFS-DGEFFS, RD-054-2016-SERFOR-DGSPFFS). The University of  
736 Georgia Advanced Computing Resource Center provided computational  
737 resources. Funding was provided by the National Science Foundation (Grant  
738 DEB-1020966) to DS and SA and the Pan American Health Organization to  
739 WV. DS was funded by a Sir Henry Dale Fellowship, jointly funded by the  
740 Wellcome Trust and Royal Society (Grant 102507/Z/13/Z). The findings and  
741 the conclusions in this report are those of the authors and do not necessarily  
742 represent the official position of Centers for Disease Control and Prevention,  
743 Atlanta, GA, USA..

- 744 1. Plowright RK, et al. (2014) Ecological dynamics of emerging bat virus spillover. *Proc Roy Soc B*. doi:10.1098/rspb.2014.2124.
- 745 2. Altizer S, Bartel R, Han BA (2011) Animal migration and infectious disease risk. *Science* 331(6015):296–302.
- 746 3. Mazé-Guilmo E, Blanchet S, McCoy KD, Loot G (2016) Host dispersal as the driver of parasite genetic structure: A paradigm lost? *Ecol Lett*:336–347.
- 747 4. Biek R, Drummond AJ, Poss M (2006) A virus reveals population structure and recent demographic history of its carnivore host. *Science* 311(5760):538–41.
- 748 5. Turmelle AS, Kunz TH, Sorenson MD (2011) A tale of two genomes: contrasting patterns of phylogeographic structure in a widely distributed bat. *Mol Ecol* 20(2):357–75.
- 749 6. Zink RM, Barrowclough GF (2008) Mitochondrial DNA under siege in avian phylogeography. *Mol Ecol* 17(9):2107–2121.
- 750 7. Johnson N, Aréchiga-Ceballos N, Aguilar-Setien A (2014) Vampire bat rabies: ecology, epidemiology and control. *Viruses* 6(5):1911–1928.
- 751 8. WHO (2013) WHO Expert Consultation on Rabies: Second Report. *Tech Rep Ser* 982:1–139.
- 752 9. Linhart SB, Mitchell GC, Crespo RF (1972) Control of vampire bats by topical application of an anticoagulant (chlorophacinone). *Bol La Of Sanit Panam* 73(2):31–38.
- 753 10. Blackwood JC, Streicker DG, Altizer S, Rohani P (2013) Resolving the roles of immunity, pathogenesis, and immigration for rabies persistence in vampire bats. *Proc Natl Acad Sci U S A*. doi:10.1073/pnas.1308817110.
- 754 11. Benavides JA, Valderrama W, Streicker DG (2016) Spatial expansions and travelling waves of rabies in vampire bats. *Proc R Soc B Biol Sci* 283(1832). doi:10.1098/rspb.2016.0328.
- 755 12. Martins FM, Templeton AR, Pavan ACO, Kohlbach BC, Morgante JS (2009) Phylogeography of the common vampire bat (*Desmodus rotundus*): Marked population structure, Neotropical Pleistocene vicariance and incongruence between nuclear and mtDNA markers. *BMC Evol Biol* 9(294). doi:10.1186/1471-2148-9-294.
- 756 13. Romero-Navia C, León-Paniagua L, Ortega J (2014) Microsatellites loci reveal heterozygosity and population structure in vampire bats (*Desmodus rotundus*) (*Chiroptera: Phyllostomidae*) of Mexico. *Rev Biol Trop* 62(2):659–69.
- 757 14. Condiri-Condiri RE, Streicker DG, Cabezas-Sanchez C, Velasco-Villa A (2013) Enzootic and epizootic rabies associated with vampire bats, Peru. *Emerg Infect Dis* 19(9):1463–1469.
- 758 15. Torres C, et al. (2014) Phylodynamics of vampire bat-transmitted rabies in Argentina. *Mol Ecol* 23(9):2340–2352.
- 759 16. Loveridge AJ, Macdonald DW (2001) Seasonality in spatial organization and dispersal of sympatric jackals (*Canis mesomelas* and *C. adustus*): implications for rabies management. *J Zool* 253(2001):101–111.
- 760 17. Craft ME, Volz E, Packer C, Meyers LA (2011) Disease transmission in territorial populations: the small-world network of Serengeti lions. *J R Soc Interface* 8(59):776–786.
- 761 18. Greenwood PJ (1980) Mating systems, philopatry and dispersal in birds and mammals. *Anim Behav* 28(4):1140–1162.
- 762 19. Wilkinson GS (1985) The social organization of the common vampire bat: II Mating system, genetic structure and relatedness. *Behav Ecol Sociobiol* 17:123–134.
- 763 20. Melnick DJ, Hoelzel GA (1992) Differences in male and female macaque dispersal lead to contrasting distributions of nuclear and mitochondrial DNA variation. *Int J Primatol* 13(4):379–393.
- 764 21. GouDET J, Perrin N, Waser P (2002) Tests for sex-biased dispersal using bi-parentally inherited genetic markers. *Mol Ecol* 11(6):1103–1114.
- 765 22. Moreno JA, Baer GM (1980) Experimental rabies in the vampire bat. *Am J Trop Med Hyg* 29(2):254–259.
- 766 23. Lord RD (1992) Seasonal reproduction of vampire bats and its relation to seasonality of bovine rabies. *J Wildl Dis* 28(2):292–294.
- 767 24. Nunn CL, Thrall PH, Stewart K, Harcourt AH (2008) Emerging infectious diseases and animal social systems. *Evol Ecol* 22(4):519–543.
- 768 25. Navarro AM, Bustamante J, Sato A (2007) Situación actual y control de la rabia en el Perú. *Rev Peru Med Exp Salud Publica* 24(1):46–50.
- 769 26. Quintana H, Pacheco V (2007) Identificación y distribución de los murciélagos vampiros del Perú. *Rev Peru Med Exp Salud Publica* 24:81–88.
- 770 27. Streicker DG, et al. (2010) Host phylogeny constrains cross-species emergence and establishment of rabies virus in bats. *Science* 329(5992):676–679.
- 771 28. Catenazzi A, Donnelly MA (2008) Sea lion (*Otaria flavescens*) as host of the common vampire bat (*Desmodus rotundus*). *Mar Ecol Prog Ser* 360:285–289.
- 772 29. Fornes A, et al. (1974) Control of bovine rabies through vampire bat control. *J Wildl Dis* 10(4):310.
- 773 30. Pope LC, et al. (2007) Genetic evidence that culling increases badger movement: Implications for the spread of bovine tuberculosis. *Mol Ecol* 16(23):4919–4929.
- 774 31. Hafner MS, et al. (1994) Disparate rates of molecular evolution in cospeciating host and parasites. *Science* 265(5175):1087–1090.
- 775 32. Zwickl DJ, Hills DM (2006) Genetic algorithm approaches for the phylogenetic analysis of large biological sequence datasets under the maximum likelihood criterion. Dissertation (The University of Texas at Austin, Austin).
- 776 33. Drummond AJ, Suchard MA, Xie D, Rambaut A (2012) Bayesian phylogenetics with BEAUti and the BEAST 1.7. *Mol Biol Evol* 29(8):1969–1973.
- 777 34. Darriba D, Taboada GL, Doallo R, Posada D (2012) jModelTest 2: more models, new heuristics and parallel computing. *Nat Methods* 9(8):772.
- 778 35. Baele G, et al. (2012) Improving the accuracy of demographic and molecular clock model comparison while accommodating phylogenetic uncertainty. *Mol Biol Evol* 29(9):2157–2167.
- 779 36. Lemey P, Rambaut A, Welch JJ, Suchard MA (2010) Phylogeography takes a relaxed random walk in continuous space and time. *Mol Biol Evol* 27(8):1877–1885.
- 780 37. Dellicour S, Rose R, Pybus OG (2016) Explaining the geographic spread of emerging viruses: a new framework for comparing viral genetic information and environmental landscape data. *BMC Bioinformatics* 17(82):1–12.
- 781 38. Paradis E (2010) *pegas*: an R package for population genetics with an integrated – modular approach. *Bioinformatics* 26(3):419–420.
- 782 39. Pritchard JK, Stephens M, Donnelly P (2000) Inference of population structure using multilocus genotype data. *Genetics* 155(2):945–959.
- 783 40. Jombart T, Devillard S, Balloux F (2010) Discriminant analysis of principal components: a new method for the analysis of genetically structured populations. *BMC Genet* 11(1):94.